Superdirective Beamforming Based on the Krylov Matrix

Gongping Huang, *Student Member, IEEE*, Jacob Benesty, and Jingdong Chen, *Senior Member, IEEE*

***Abstract*—Superdirective beamforming has attracted a significant amount of research interest in speech and audio applications, since it can maximize the directivity factor (DF) given an array geometry and, therefore, is efficient in dealing with signal acquisition in diffuse-like noise environments. However, this beamformer is very sensitive to sensor self-noise and mismatch among sensors, which considerably restricts its use in practical systems. This paper develops an approach to superdirective beamforming based on the Krylov matrix. We show that the columns of a proposed Krylov matrix, which span a chosen dimension of the whole space, are interesting beamformers; consequently, all different linear combinations of those columns lead to beamformers that have good properties. In particular, we develop the Krylov maximum white noise gain and Krylov maximum DF beamformers, which are obtained by maximizing the WNG and the DF, respectively. By properly choosing the dimension of the Krylov subspace, the developed beamformers that can make a compromise between reasonable values of the DF and white noise amplification. We also extend the basic idea to the design of the Krylov maximum front-to-back ratio, parametric superdirective, and parametric supercardioid beamformers.**

***Index Terms*—Directivity factor, front-to-back ratio, hypercardioid, Krylov matrix, microphone arrays, robust beamforming, superdirective beamforming, supercardioid, white noise gain.**

I. Introduction

In VOICE communications and human-machine interfaces, the signal of interest (or desired signal) picked up by microphones is inevitably contaminated by unwanted interferences and noises, such as additive noise, competing sources, and convolutive noise. This problem has been intensively investigated over the past few decades. Many approaches have been developed [1]–[8] and most of which involve the use of microphone arrays. Consequently, the design of microphone arrays and the associated processing algorithms have attracted a significant amount of interest in the literature [4], [9]–[16]. Besides the selection of sensors and array geometry as well as the design of multichannel analogue-to-digital (A/D) converters, the critical component of a microphone system is the so-called beamforming [17]–[20], which basically forms a spatial filter that is able to extract signals from a certain look direction while suppressing signals and noise from other directions. Many beamforming algorithms have been developed so far, such as the delay-and-sum (DS) [21], [22], filter-and-sum (FS) [2], [23], superdirective [1], [24], [25], differential [26], [27], [29], [30], and adaptive beamformers [2], [9], [23], [35].

The core issue of beamforming is to determine the coefficients of the beamforming filter, which are applied to the microphones' outputs. Depending on how these filters are designed, beamforming algorithms can be categorized into two fundamental classes: fixed and adaptive. The former maintains a fixed spatial response (beampattern) once the array is deployed, which is independent of the array observation data [27], [31], [32]. The representative beamformers in this class include the well-known DS, superdirective [1], [3], [25], [33], and differential ones [26], [27], [29], [30]. In contrast, adaptive beamformers update their coefficients according to either the array outputs or the noise statistics, so their beampatterns vary with the environment. Popular algorithms in this category include the minimum variance distortionless response (MVDR) [2] and linearly constrained minimum variance (LCMV) filters [9], [23], [35]. Generally speaking, adaptive beamformers can be more efficient than fixed ones in suppressing noise and reverberation. However, the estimation of the signal and noise statistics plays a paramount role in their performance. If those statistics are not estimated accurately, the estimation errors can cause desired signal cancellation and distortion. In many applications, fixed beamformers are very attractive because of their performance stability and also low computational complexity and ease of real-time implementation since their filters' coefficients can be pre-calculated and loaded into the system. This paper focusses on fixed beamformers with small-size microphone arrays.

With small-size microphone arrays, one of the most critical issues is how to deal with signal acquisition in reverberant environments where a large number of reflections tend to form an acoustic field that is close to a spherically isotropic (diffuse) noise field (noise with equal energy that propagates from all directions). In this scenario, two evaluation measures are important: the directivity factor (DF) and the front-to-back ratio (FBR). The superdirective beamformer is generally derived by maximizing the DF [1], [34], [36], [37]. Besides achieving the maximum value of the DF, another great property of the superdirective beamformer is that its beampattern is frequency invariant, which makes this beamformer appropriate for processing acoustic and audio signals whose frequencies may range from a few Hz to more than 20 kHz. However, this beamformer is very sensitive to array imperfections which considerably restricts its use in practical systems [33], [38]. A good measure of this sensitivity is the so-called white noise gain (WNG) [27], [28]. A

Manuscript received April 7, 2016; revised August 13, 2016 and October 11, 2016; accepted October 12, 2016. Date of publication October 18, 2016; date of current version November 4, 2016. This work was supported in part by the NSFC Distinguished Young Scientists Fund under Grant 61425005. The work of G. Huang was supported in part by the China Scholarship Council. The associate editor coordinating the review of this manuscript and approving it for publication was Dr. Richard Christian Hendriks.

G. Huang is with the Center of Intelligent Acoustics and Immersive Communications, School of Marine Science and Technology, Northwestern Polytechnical University, Xi'an 710072, China, and also with the INRS-EMT, University of Quebec, Montreal, QC H5A1K6, Canada (e-mail: gongpinghuang@gmail.com).

J. Benesty is with the INRS-EMT, University of Quebec, Montreal, QC H5A 1K6, Canada (e-mail: benesty@emt.inrs.ca).

J. Chen is with the Center of Intelligent Acoustics and Immersive Communications, Northwestern Polytechnical University, Xi'an 710072, China (e-mail: jingdongchen@ieee.org).

Color versions of one or more of the figures in this paper are available online at http://ieeexplore.ieee.org.

Digital Object Identifier 10.1109/TASLP.2016.2618003

negative value (in dB) of the WNG means white noise amplification. For the superdirective beamformer, the WNG can be very low at low frequencies, indicating significant white noise amplification at those frequencies.

When the microphone array spacing is small, it has been shown that the superdirective beamformer corresponds to the hypercardioid since the latter is, by its own definition, obtained also by maximizing the DF [27]. In some applications, it is more interesting to maximize the FBR, which leads to a beamformer with a supercardioid pattern. This beamformer, however, also suffers from significant white noise amplification but somewhat less than the superdirective beamformer. Therefore, how to achieve a relatively high DF (or FBR) with a reasonable WNG is an important issue regarding the design of superdirective and supercardioid beamformers.

Much research has been conducted in the literature to deal with the problem of white noise amplification. One of the most used solutions is the so-called regularized superdirective beamformer [17], [30], [33], [39], which introduces a WNG constraint to improve robustness. The performance of this beamformer is controlled by a regularization parameter [17]. While it can improve the beamformer's robustness with respect to array imperfection, how to find a proper value of the regularization parameter is not a trivial issue as it is frequency dependent. Moreover, regularization makes the beampattern and DF of the superdirective beamformer change with frequency, which can lead to signal distortion when applied to broadband acoustic and audio signals. Alternative approaches were also developed to deal with the problem of white noise amplification [40]–[43], such as the probability based, nonlinear optimization based, combined [44], and subspace beamformers [45]. The work in [44] combines the regularized superdirective beamformer and the DS one, resulting in a robust regularized superdirective beamformer, which can make a performance tradeoff between the DF and the WNG. In [45], the problem of superdirective beamforming is expressed with a joint diagonalization method and a subspace superdirective beamformer is derived, which achieves a compromise between a high value of the DF and a proper level of white noise amplification.

Despite the efforts that have been made, white noise amplification remains a challenging problem for superdirective beamforming. Further study is indispensable. In this paper, we investigate the problem of white noise amplification in superdirective beamforming based on the Krylov matrix [46]. The Krylov matrix [46], which is in relation to the eigenvalues of large linear systems, has a great potential in beamforming. There has already been some discussions on the application of this matrix in adaptive beamforming. For example, the work in [47] analyzed the performance of the Krylov subspace-based dimensionality reduction for adaptive beamforming. In [48], the orthogonal Krylov subspace was used in a reduced dimensional subspace to estimate the steering vector mismatch. In [49] and [50], the orthogonal Krylov subspace was used in deriving robust adaptive beamformers. In this paper, we show that the columns of a proposed Krylov matrix, which span a certain dimension of the entire space, are interesting beamformers. For instance, the first and last columns correspond to the well-known DS and superdirective beamformers, and the other columns are beamformers that can make a compromise between the WNG and the DF. Different linear combinations of the columns of the Krylov matrix can form many beamformers with interesting properties. In particular, we propose the Krylov maximum WNG (KMWNG) and the Krylov maximum DF (KMDF) beamformers, which can compromise between the DF and the WNG by adjusting the dimension of the Krylov subspace. We also extend the basic idea to the design of the Krylov supercardioid, parametric superdirective beamformer, and parametric supercardioid.

The major contributions of this paper are as follows. 1) It presents an approach to the design of the superdirective and supercardiod beamformers based on a proposed matrix, which can be easily generalized to the design of many other beampatterns. 2) It develops parametric superdirective and supercardioid beamformers, which can be viewed as a generalization of the work in [44] that combines the superdirective beamformer together with the DS beamformer to create a robust superdirective beamformer. 3) It presents some alternatives to the robust superdirective and supercardioid beamformers. These alternatives provide more flexible choices to design superdirective beamformers in practical systems.

The rest of this paper is organized as follows. In Section II, we explain the signal model and the problem of beamforming with uniform linear arrays (ULAs). Section III presents some performance measures that are used to derive and/or evaluate different kinds of fixed beamformers. Section IV gives the most well-known and studied fixed beamformers. In Sections V and Section VI, we derive the Krylov superdirective beamformer and the Krylov supercardioid. In Section VII and Section VIII, we discuss the parametric superdirective beamformer and the parametric supercardioid. Section IX presents some simulation results to validate the theoretical derivations. Finally, we give our conclusions in Section X.

II. Signal Model and Problem Formulation

We consider a ULA consisting of M omnidirectional microphones, where the distance between two successive sensors is equal to δ. A source signal (plane wave), in the farfield, impinges on the ULA from the direction (azimuth angle) θ, at the speed of sound, e.g., $c = 340$ m/s. In this scenario, the steering vector (of length M) is

$$\mathbf{d}(\omega,\theta) \triangleq \left[1 \; e^{-\jmath\omega\tau_0\cos\theta} \; \cdots \; e^{-\jmath(M-1)\omega\tau_0\cos\theta}\right]^T, \quad (1)$$

where the superscript ^{T} is the transpose operator, $\jmath$ is the imaginary unit with $\jmath^2 = -1$, $\omega = 2\pi f$ is the angular frequency, $f > 0$ is the temporal frequency, and $\tau_0 = \delta/c$ is the delay between two successive sensors at the angle $\theta = 0$.

In order to avoid spatial aliasing [3], it is necessary that the interelement spacing is less than $\lambda/2$, where λ is the acoustic wavelength. In this paper, we consider fixed beamformers with small values of δ, so that this condition easily holds. We also assume that the desired signal comes from the endfire direction, i.e., $\theta = 0$. (Note that with ULAs, the performance of the superdirective beamformer is a function of the source incidence angle with its best performance appearing at endfire directions [51]; so this beamformer may not be able to be steered properly in all directions.) Then, the received signal at the mth ($m = 1, 2, \ldots, M$) microphone in the frequency domain is

$$\begin{aligned} Y_m(\omega) &= e^{\jmath(m-1)\omega\tau_0} X(\omega) + V_m(\omega) \\ &= X_m(\omega) + V_m(\omega), \end{aligned} \quad (2)$$

where $X(\omega)$ is the desired signal, and $X_m(\omega)$ and $V_m(\omega)$ are the delayed version of the desired signal and additive noise at the

mth microphone, respectively. In a vector notation, (2) becomes

$$\begin{aligned}\mathbf{y}(\omega) &\triangleq \mathbf{x}(\omega)+\mathbf{v}(\omega)\\ &= \mathbf{d}(\omega)X(\omega)+\mathbf{v}(\omega),\end{aligned} \tag{3}$$

where

$$\begin{aligned}\mathbf{y}(\omega) &\triangleq [\,Y_1(\omega)\quad Y_2(\omega)\quad\cdots\quad Y_M(\omega)\,]^T,\\ \mathbf{x}(\omega) &\triangleq [\,X_1(\omega)\quad X_2(\omega)\quad\cdots\quad X_M(\omega)\,]^T\\ &= \mathbf{d}(\omega)X(\omega),\\ \mathbf{v}(\omega) &\triangleq [\,V_1(\omega)\quad V_2(\omega)\quad\cdots\quad V_M(\omega)\,]^T,\end{aligned} \tag{4}$$

and $\mathbf{d}(\omega)=\mathbf{d}(\omega,0)$ is the signal propagation vector.

The objective of beamforming is to recover the desired signal, $X(\omega)$, from the noisy observation vector, $\mathbf{y}(\omega)$. To do that, a complex weight, $H_m^*(\omega)$ $(m=1,2,\ldots,M)$, where the superscript * is the complex conjugate, is applied at the output of the mth microphone. The weighted outputs are then summed together to get an estimate of the desired signal [9], i.e.,

$$\begin{aligned}Z(\omega) &= \sum_{\mathrm{m}=1}^{M} H_m^*(\omega)Y_m(\omega)\\ &= \mathbf{h}^H(\omega)\mathbf{y}(\omega)\\ &= \mathbf{h}^H(\omega)\mathbf{d}(\omega)X(\omega)+\mathbf{h}^H(\omega)\mathbf{v}(\omega),\end{aligned} \tag{5}$$

where

$$\mathbf{h}(\omega)\triangleq [\,H_1(\omega)\quad H_2(\omega)\quad\cdots\quad H_M(\omega)\,]^T \tag{6}$$

is a spatial filter of length M and the superscript ^{H} is the conjugate-transpose operator. In our context, the distortionless constraint at the desired direction, $\theta=0$, is desired, i.e.,

$$\mathbf{h}^H(\omega)\mathbf{d}(\omega)=1. \tag{7}$$

III. Performance Measures

In this work, we use the following performance measures for the derivation and/or evaluation of different kind of fixed beamformers.

A. Beampattern

The beampattern or directivity pattern describes the sensitivity of the beamformer to a plane wave impinging on the array from the direction θ. Mathematically, it is defined as

$$\begin{aligned}\mathcal{B}[\mathbf{h}(\omega),\theta] &\triangleq \mathbf{h}^H(\omega)\mathbf{d}(\omega,\theta)\\ &= \sum_{\mathrm{m}=1}^{M} H_m^*(\omega)e^{-\jmath(m-1)\omega\tau_0\cos\theta}.\end{aligned} \tag{8}$$

B. Front-to-Back Ratio

The FBR is defined as the ratio of power gain between the front and rear of the beampattern, i.e., [3]

$$\begin{aligned}\mathcal{F}[\mathbf{h}(\omega)] &\triangleq \frac{\int_0^{\pi/2}|\mathcal{B}[\mathbf{h}(\omega),\theta]|^2\sin\theta d\theta}{\int_{\pi/2}^{\pi}|\mathcal{B}[\mathbf{h}(\omega),\theta]|^2\sin\theta d\theta}\\ &= \frac{\mathbf{h}^H(\omega)\mathbf{\Gamma}_{0,\pi/2}(\omega)\mathbf{h}(\omega)}{\mathbf{h}^H(\omega)\mathbf{\Gamma}_{\pi/2,\pi}(\omega)\mathbf{h}(\omega)},\end{aligned} \tag{9}$$

where

$$\mathbf{\Gamma}_{0,\pi/2}(\omega) \triangleq \int_0^{\pi/2}\mathbf{d}(\omega,\theta)\mathbf{d}^H(\omega,\theta)\sin\theta d\theta, \tag{10}$$

$$\mathbf{\Gamma}_{\pi/2,\pi}(\omega) \triangleq \int_{\pi/2}^{\pi}\mathbf{d}(\omega,\theta)\mathbf{d}^H(\omega,\theta)\sin\theta d\theta. \tag{11}$$

It can be verified that the elements of these matrices are

$$\left[\mathbf{\Gamma}_{0,\pi/2}(\omega)\right]_{ij} = \begin{cases}\dfrac{e^{\jmath\omega(j-i)\tau_0}-1}{\jmath\omega(j-i)\tau_0}, & i\neq j\\ 1, & i=j\end{cases} \tag{12}$$

$$\left[\mathbf{\Gamma}_{\pi/2,\pi}(\omega)\right]_{ij} = \begin{cases}\dfrac{1-e^{-\jmath\omega(j-i)\tau_0}}{\jmath\omega(j-i)\tau_0}, & i\neq j\\ 1, & i=j\end{cases}, \tag{13}$$

respectively, with $i,j=1,2,\ldots,M$.

C. Signal-to-Noise Ratio Gains

Without loss of generality, we consider the first microphone as the reference. The input SNR is then defined as

$$\mathrm{iSNR}(\omega)\triangleq\frac{\phi_X(\omega)}{\phi_{V_1}(\omega)}, \tag{14}$$

where $\phi_X(\omega)\triangleq E\left[|X(\omega)|^2\right]$ and $\phi_{V_1}(\omega)\triangleq E\left[|V_1(\omega)|^2\right]$ are the variances of $X(\omega)$ and $V_1(\omega)$, respectively, with $E[\cdot]$ denoting mathematical expectation. The output SNR is given by

$$\begin{aligned}\mathrm{oSNR}[\mathbf{h}(\omega)] &= \phi_X(\omega)\times\frac{\left|\mathbf{h}^H(\omega)\mathbf{d}(\omega)\right|^2}{\mathbf{h}^H(\omega)\mathbf{\Phi}_{\mathbf{v}}(\omega)\mathbf{h}(\omega)}\\ &= \frac{\phi_X(\omega)}{\phi_{V_1}(\omega)}\times\frac{\left|\mathbf{h}^H(\omega)\mathbf{d}(\omega)\right|^2}{\mathbf{h}^H(\omega)\mathbf{\Gamma}_{\mathbf{v}}(\omega)\mathbf{h}(\omega)},\end{aligned} \tag{15}$$

where $\mathbf{\Phi}_{\mathbf{v}}(\omega)\triangleq E\left[\mathbf{v}(\omega)\mathbf{v}^H(\omega)\right]$ and $\mathbf{\Gamma}_{\mathbf{v}}(\omega)\triangleq\dfrac{\mathbf{\Phi}_{\mathbf{v}}(\omega)}{\phi_{V_1}(\omega)}$ are the correlation and pseudo-coherence matrices [54] of $\mathbf{v}(\omega)$, respectively. The definition of the SNR gain is obtained from the previous SNR definitions, i.e.,

$$\begin{aligned}\mathcal{G}[\mathbf{h}(\omega)] &\triangleq \frac{\mathrm{oSNR}[\mathbf{h}(\omega)]}{\mathrm{iSNR}(\omega)}\\ &= \frac{\left|\mathbf{h}^H(\omega)\mathbf{d}(\omega)\right|^2}{\mathbf{h}^H(\omega)\mathbf{\Gamma}_{\mathbf{v}}(\omega)\mathbf{h}(\omega)}.\end{aligned} \tag{16}$$

In our discussion, we are interested in two types of noise.

1) The temporally and spatially white noise with the same variance at all microphones.[1] In this case, $\mathbf{\Gamma_v}(\omega) = \mathbf{I}_M$, where $\mathbf{I}_M$ is the $M \times M$ identity matrix. Therefore, the SNR gain is

$$\mathcal{W}[\mathbf{h}(\omega)] = \frac{\left|\mathbf{h}^H(\omega)\,\mathbf{d}(\omega)\right|^2}{\mathbf{h}^H(\omega)\,\mathbf{h}(\omega)}, \tag{17}$$

which is called the white noise gain (WNG) [11].

2) The spherically isotropic noise. In this case, the noise pseudo-coherence matrix is

$$\begin{aligned}[\mathbf{\Gamma_v}(\omega)]_{ij} &= [\mathbf{\Gamma}(\omega)]_{ij} = \frac{\sin[\omega(j-i)\tau_0]}{\omega(j-i)\tau_0} \\ &= \operatorname{sinc}[\omega(j-i)\tau_0], \end{aligned} \tag{18}$$

with $i, j = 1, 2, \ldots, M$. Now, the SNR gain is

$$\mathcal{D}[\mathbf{h}(\omega)] = \frac{\left|\mathbf{h}^H(\omega)\,\mathbf{d}(\omega)\right|^2}{\mathbf{h}^H(\omega)\,\mathbf{\Gamma}(\omega)\,\mathbf{h}(\omega)}, \tag{19}$$

which is called the directivity factor (DF) [3].

IV. Conventional Fixed Beamformers

In this section, we briefly discuss the most studied fixed beamformers with microphone arrays.

The DS beamformer is given by

$$\mathbf{h}_{\mathrm{DS}}(\omega) = \frac{\mathbf{d}(\omega)}{M}. \tag{20}$$

This beamformer leads to the maximum WNG, which is $\mathcal{W}[\mathbf{h}_{\mathrm{DS}}(\omega)] = M$.

The superdirective beamformer, which is generally derived from the maximization of the DF [1], [27], is given by

$$\mathbf{h}_{\mathrm{SD}}(\omega) = \frac{\mathbf{\Gamma}^{-1}(\omega)\,\mathbf{d}(\omega)}{\mathbf{d}^H(\omega)\,\mathbf{\Gamma}^{-1}(\omega)\,\mathbf{d}(\omega)}. \tag{21}$$

This beamformer leads to the maximum value of the DF, which is $\mathcal{D}[\mathbf{h}_{\mathrm{SD}}(\omega)] = \mathbf{d}^H(\omega)\,\mathbf{\Gamma}^{-1}(\omega)\,\mathbf{d}(\omega)$ and this value is close to M^2 if the spacing δ is small [52]. In fact, when the microphone array size is very small, the superdirective beamformer corresponds to the hypercardioid of order $M-1$ [27]. It is well known that $\mathbf{h}_{\mathrm{SD}}(\omega)$ is very sensitive to sensor noise and array imperfections.

The robust (or regularized) superdirective beamformer, which is obtained from the maximization of the DF with a constraint on the WNG, is [17]

$$\mathbf{h}_{\mathrm{R},\epsilon}(\omega) = \frac{\left[\mathbf{\Gamma}(\omega) + \epsilon\mathbf{I}_M\right]^{-1}\mathbf{d}(\omega)}{\mathbf{d}^H(\omega)\left[\mathbf{\Gamma}(\omega) + \epsilon\mathbf{I}_M\right]^{-1}\mathbf{d}(\omega)}, \tag{22}$$

where $\epsilon \geq 0$ is the regularization parameter. The parameter ϵ tries to find a good compromise between a large DF and white noise amplification. A small value of ϵ leads to a large DF but a low WNG, while a large value of ϵ gives a large WNG but a low DF. Two interesting cases of (22) are $\mathbf{h}_{\mathrm{R},0}(\omega) = \mathbf{h}_{\mathrm{SD}}(\omega)$ and $\mathbf{h}_{\mathrm{R},\infty}(\omega) = \mathbf{h}_{\mathrm{DS}}(\omega)$. While regularization can help improve the WNG, finding the proper value of the parameter ϵ in practical microphone array systems is not a trivial issue as it depends on the frequency, the sensor quality, the mismatch between sensors, and the sensor spacing as well.

The supercardioid beamformer is deduced by maximizing the FBR defined in (9) [3]. The solution is obtained by solving the generalized eigenvalue problem (GEP):

$$\mathbf{\Gamma}_{0,\pi/2}(\omega)\,\mathbf{t}(\omega) = \lambda(\omega)\,\mathbf{\Gamma}_{\pi/2,\pi}(\omega)\,\mathbf{t}(\omega). \tag{23}$$

Denoting $\lambda_1(\omega)$ the largest eigenvalue of this GEP with $\mathbf{t}_1(\omega)$ the corresponding eigenvector, and using the distortionless constraint, we find that the supercardioid of order $M-1$ is

$$\mathbf{h}_{\mathrm{SC}}(\omega) = \frac{\mathbf{t}_1(\omega)}{\mathbf{d}^H(\omega)\,\mathbf{t}_1(\omega)}, \tag{24}$$

which leads to the maximum FBR, i.e., $\mathcal{F}[\mathbf{h}_{\mathrm{SC}}(\omega)] = \lambda_1(\omega)$. This beamformer also suffers from the problem of white noise amplification.

The objective of this paper is to find other alternatives to the robust superdirective and supercardioid beamformers and ways to compromise between the WNG and the DF (or FBR).

In the following, for ease of exposition, we will drop ω from all the variables whenever there is no ambiguity.

V. Krylov Superdirective Beamformer

Using the well-known eigenvalue decomposition [53], the pseudo-coherence matrix of the diffuse noise can be decomposed as

$$\mathbf{\Gamma} = \mathbf{U}\mathbf{\Lambda}\mathbf{U}^T, \tag{25}$$

where $\mathbf{U}$ is an orthogonal matrix, i.e., $\mathbf{U}^T\mathbf{U} = \mathbf{U}\mathbf{U}^T = \mathbf{I}_M$, and $\mathbf{\Lambda}$ is a diagonal matrix whose main elements are strictly positive as $\mathbf{\Gamma}$ is positive definite. From this decomposition, it is then easy to compute

$$\mathbf{\Gamma}^{-\frac{1}{M-1}} = \mathbf{U}\mathbf{\Lambda}^{-\frac{1}{M-1}}\mathbf{U}^T. \tag{26}$$

Given $\mathbf{\Gamma}^{-\frac{1}{M-1}}$ and letting $1 \leq N \leq M$, the $M \times N$ Krylov matrix of $\mathbf{\Gamma}^{-\frac{1}{M-1}}$ generated by the vector $\mathbf{d}$ is defined as [46]

$$\begin{aligned}\mathbf{K}_N &= \left[\mathbf{k}_1 \quad \mathbf{k}_2 \quad \cdots \quad \mathbf{k}_{N-1} \quad \mathbf{k}_N\right] \\ &= \left[\mathbf{d} \quad \mathbf{\Gamma}^{-\frac{1}{M-1}}\mathbf{d} \quad \cdots \quad \mathbf{\Gamma}^{-\frac{N-2}{M-1}}\mathbf{d} \quad \mathbf{\Gamma}^{-\frac{N-1}{M-1}}\mathbf{d}\right], \end{aligned} \tag{27}$$

where $\mathbf{k}_m = \mathbf{\Gamma}^{-\frac{m-1}{M-1}}\mathbf{d}$ with $m = 1, 2, \ldots, N$. In general, $\mathbf{K}_N$ is a rectangular matrix; but it becomes a square one if $N = M$.

With the steering vector $\mathbf{d}$ and the two matrices $\mathbf{\Gamma}$ and $\mathbf{K}_N$, we have the following properties.

Property 5.1: $\mathbf{d}$ is not an eigenvector of $\mathbf{\Gamma}$.

Proof: Let us prove this property by contradiction. Suppose that $\mathbf{d}$ is an eigenvector of $\mathbf{\Gamma}$, then we should have

$$\mathbf{\Gamma}\mathbf{d} = \lambda\mathbf{d}, \tag{28}$$

where $\lambda \neq 0$. Since $\mathbf{\Gamma}$ is a positive definite matrix, it follows immediately that

$$\mathbf{\Gamma}^{-1}\mathbf{d} = \frac{1}{\lambda}\mathbf{d}. \tag{29}$$

Substituting (29) into the superdirective beamformer, we obtain

$$\mathbf{h}_{\mathrm{S}} = \frac{1}{M}\mathbf{d} = \mathbf{h}_{\mathrm{DS}}. \tag{30}$$

[1] This noise models well the sensor noise.

This apparently contradicts with the fact that $\mathbf{h}_{\mathrm{S}} \neq \mathbf{h}_{\mathrm{DS}}$. Therefore, $\mathbf{d}$ should not be an eigenvector of $\mathbf{\Gamma}$, which completes the proof. ■

Property 5.2: $\mathbf{K}_N$ is a full-column rank matrix.

Proof: Using Property 5.1, we can verify that $\mathbf{d}$ is neither an eigenvector of $\mathbf{\Gamma}^{-\frac{m}{M-1}}$, where $m \in \{1, 2, \ldots, N-1\}$ nor an eigenvector of any linear combination of all the $N-1$ matrices $\mathbf{\Gamma}^{-\frac{m}{M-1}}$ with $m = 1, 2, \ldots, N-1$. It follows then that any column vector of the $\mathbf{K}_N$ matrix, i.e., $\mathbf{k}_m$, $m \in \{1, 2, \ldots, N-1\}$, cannot be written as a linear combination of the other column vectors. Therefore, $\mathbf{K}_N$ is a full-column rank matrix. ■

For $N = M$, $\mathbf{K}_N$ becomes the following square matrix:

$$\begin{aligned}\mathbf{K}_M &= \left[\mathbf{d} \quad \mathbf{\Gamma}^{-\frac{1}{M-1}}\mathbf{d} \quad \cdots \quad \mathbf{\Gamma}^{-\frac{M-2}{M-1}}\mathbf{d} \quad \mathbf{\Gamma}^{-1}\mathbf{d}\right] \\ &= \left[\mathbf{k}_1 \quad \mathbf{k}_2 \quad \cdots \quad \mathbf{k}_{\mathrm{M}-1} \quad \mathbf{k}_M\right].\end{aligned} \tag{31}$$

The columns of $\mathbf{K}_M$, which span the whole space, are good beamformers. Indeed, the first (normalized) column of $\mathbf{K}_M$ is the DS beamformer:

$$\frac{\mathbf{k}_1}{\mathbf{d}^H\mathbf{k}_1} = \mathbf{h}_{\mathrm{DS}}, \tag{32}$$

the last (normalized) column of $\mathbf{K}_M$ is the superdirective beamformer:

$$\frac{\mathbf{k}_M}{\mathbf{d}^H\mathbf{k}_M} = \mathbf{h}_{\mathrm{SD}}, \tag{33}$$

while the other (normalized) columns are beamformers that can compromise between the WNG and the DF. In other words, the beamformer $\mathbf{k}_m$ will behave more like the superdirective beamformer as m approaches M while it will behave more like the DS beamformer when m approaches 1. As a result, we should always have

$$\mathcal{W}(\mathbf{k}_1) \geq \mathcal{W}(\mathbf{k}_2) \geq \cdots \geq \mathcal{W}(\mathbf{k}_M) \tag{34}$$

and

$$\mathcal{D}(\mathbf{k}_1) \leq \mathcal{D}(\mathbf{k}_2) \leq \cdots \leq \mathcal{D}(\mathbf{k}_M). \tag{35}$$

From these observations, it is natural to propose beamformers of the form:

$$\mathbf{h}_{\mathrm{K},N} = \mathbf{K}_N\mathbf{g}, \tag{36}$$

where

$$\mathbf{g} = \left[g_1 \quad g_2 \quad \cdots \quad g_{\mathrm{N}-1} \quad g_N\right]^T \neq \mathbf{0} \tag{37}$$

is a filter of length N. Obviously, $\mathbf{h}_{\mathrm{K},N} \in \mathrm{span}(\mathbf{K}_N)$. Taking into account the distortionless constraint, i.e.,

$$\mathbf{d}^H\mathbf{h}_{\mathrm{K},N} = \mathbf{d}^H\mathbf{K}_N\mathbf{g} = 1, \tag{38}$$

it is more convenient to consider the normalized form of (36), i.e.,

$$\mathbf{h}_{\mathrm{K},N} = \frac{\mathbf{K}_N\mathbf{g}}{\mathbf{d}^H\mathbf{K}_N\mathbf{g}}, \tag{39}$$

which we refer to as the Krylov beamformer. It is easy to verify that the elements of the vector $\mathbf{K}_N^H\mathbf{d}$ are all real. Therefore, $\mathbf{g}$ is a real-valued filter in general, which will always be assumed. The beamformer $\mathbf{h}_{\mathrm{K},N}$ in (39) can be extremely useful since one can always make a good compromise between the WNG and the DF. For example, with $\mathbf{g} = \mathbf{1}$ (the all one vector), the Krylov beamformer can be viewed as a generalization of the combined beamformer developed in [44] that combines the superdirective and DS beamformers for improved robustness with respect to white noise.

With (39), the WNG and the DF can be expressed, respectively, as

$$\mathcal{W}(\mathbf{h}_{\mathrm{K},N}) = \frac{\mathbf{g}^T\mathbf{K}_N^H\mathbf{d}\mathbf{d}^H\mathbf{K}_N\mathbf{g}}{\mathbf{g}^T\mathbf{K}_N^H\mathbf{K}_N\mathbf{g}} \tag{40}$$

and

$$\mathcal{D}(\mathbf{h}_{\mathrm{K},N}) = \frac{\mathbf{g}^T\mathbf{K}_N^H\mathbf{d}\mathbf{d}^H\mathbf{K}_N\mathbf{g}}{\mathbf{g}^T\mathbf{K}_N^H\mathbf{\Gamma}\mathbf{K}_N\mathbf{g}}. \tag{41}$$

The maximization of the WNG leads to the Krylov maximum WNG (KMWNG) beamformer:

$$\mathbf{h}_{\mathrm{KMWNG},N} = \frac{\mathbf{K}_N\left(\mathbf{K}_N^H\mathbf{K}_N\right)^{-1}\mathbf{K}_N^H\mathbf{d}}{\mathbf{d}^H\mathbf{K}_N\left(\mathbf{K}_N^H\mathbf{K}_N\right)^{-1}\mathbf{K}_N^H\mathbf{d}}. \tag{42}$$

It can be verified that $\mathbf{h}_{\mathrm{KMWNG},1} = \mathbf{h}_{\mathrm{KMWNG},M} = \mathbf{h}_{\mathrm{DS}}$. Therefore, in general, the performance of $\mathbf{h}_{\mathrm{KMWNG},N}$ is close to that of the DS beamformer.

In the same way, the maximization of the DF leads to the Krylov maximum DF (KMDF) beamformer:

$$\mathbf{h}_{\mathrm{KMDF},N} = \frac{\mathbf{K}_N\left(\mathbf{K}_N^H\mathbf{\Gamma}\mathbf{K}_N\right)^{-1}\mathbf{K}_N^H\mathbf{d}}{\mathbf{d}^H\mathbf{K}_N\left(\mathbf{K}_N^H\mathbf{\Gamma}\mathbf{K}_N\right)^{-1}\mathbf{K}_N^H\mathbf{d}}. \tag{43}$$

It is clearly seen that the performance of the KMDF beamformer depends strongly on N. By playing with the value of N, we obtain different beamformers.

1) For $N = 1$, we get the DS beamformer, i.e., $\mathbf{h}_{\mathrm{KMDF},1} = \mathbf{h}_{\mathrm{DS}}$.
2) For $N = M$, we get the superdirective beamformer, i.e., $\mathbf{h}_{\mathrm{KMDF},M} = \mathbf{h}_{\mathrm{SD}}$.
3) For $1 < N < M$, we obtain beamformers whose performances are in between the performances of the DS and superdirective beamformers.

Clearly, by properly choosing the dimension of the Krylov subspace, N, the beamformer $\mathbf{h}_{\mathrm{KMDF},N}$ can find a good compromise between a large value of the DF and white noise amplification.

VI. Krylov Supercardioid

Following the principles of the previous section, we develop a supercardioid based on the Krylov subspace. The matrices $\mathbf{\Gamma}_{0,\pi/2}$ and $\mathbf{\Gamma}_{\pi/2,\pi}$ can be decomposed as

$$\mathbf{\Gamma}_{0,\pi/2} = \mathbf{U}_1\mathbf{\Lambda}_1\mathbf{U}_1^H, \tag{44}$$

$$\mathbf{\Gamma}_{\pi/2,\pi} = \mathbf{U}_2\mathbf{\Lambda}_2\mathbf{U}_2^H, \tag{45}$$

where $\mathbf{U}_1$ and $\mathbf{U}_2$ are unitary matrices, and $\mathbf{\Lambda}_1$ and $\mathbf{\Lambda}_2$ are diagonal matrices. From these decompositions, it is then easy to compute

$$\mathbf{\Gamma}_{0,\pi/2}^{\frac{N-1}{M-1}} = \mathbf{U}_1\mathbf{\Lambda}_1^{\frac{N-1}{M-1}}\mathbf{U}_1^H, \tag{46}$$

$$\mathbf{\Gamma}_{\pi/2,\pi}^{\frac{N-1}{M-1}} = \mathbf{U}_2\mathbf{\Lambda}_2^{\frac{N-1}{M-1}}\mathbf{U}_2^H, \tag{47}$$

where $1 \leq N \leq M$.

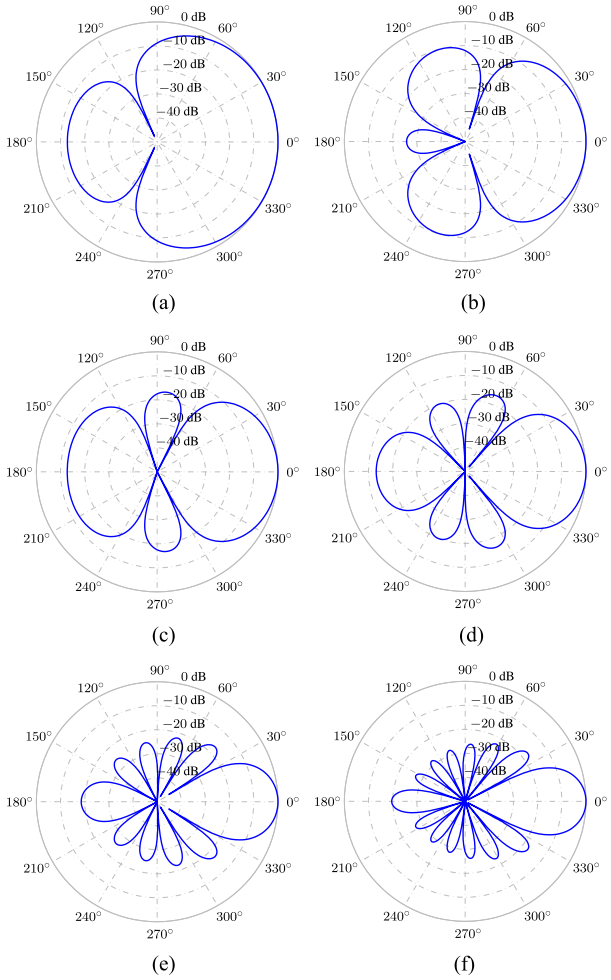

Fig. 1. Beampatterns of the KMDF beamformer with a ULA, for six different values of N: (a) $N = 1$, (b) $N = 2$, (c) $N = 3$, (d) $N = 4$, (e) $N = 6$, and (f) $N = 8$. Conditions of simulation: $M = 8$, $\delta = 1.5$ cm, and $f = 2000$ Hz.

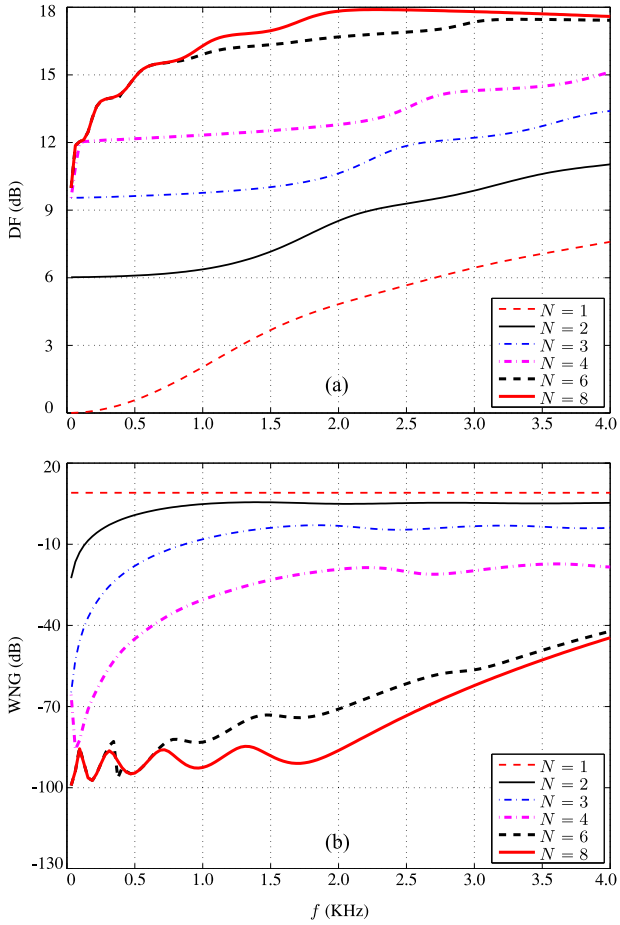

Fig. 2. DF and WNG of the KMDF beamformer with a ULA as a function of the frequency, f, for six different values of N: (a) DF and (b) WNG. Conditions of simulation: $M = 8$ and $\delta = 1.5$ cm.

Denoting $\lambda_{\mathrm{N}-1,1}$ the maximum eigenvalue of the matrix $\mathbf{\Gamma}_{\pi/2,\pi}^{-\frac{N-1}{M-1}}\mathbf{\Gamma}_{0,\pi/2}^{\frac{N-1}{M-1}}$ with $\mathbf{t}_{\mathrm{N}-1,1}$ the corresponding eigenvector, we define the $M \times N$ Krylov matrix as

$$\mathbf{T}_N = \left[\, \mathbf{t}_{0,1} \;\; \mathbf{t}_{1,1} \;\; \cdots \;\; \mathbf{t}_{\mathrm{N}-2,1} \;\; \mathbf{t}_{\mathrm{N}-1,1} \,\right]. \tag{48}$$

For $N = M$, $\mathbf{T}_N$ becomes a square matrix. The columns of $\mathbf{T}_M$, which span the whole space, are also interesting beamformers. As we did in Section V, we consider beamformers of the form:

$$\mathbf{h}_{\mathrm{K},N} = \frac{\mathbf{T}_N \mathbf{g}}{\mathbf{d}^H \mathbf{T}_N \mathbf{g}}, \tag{49}$$

where $\mathbf{g} \neq \mathbf{0}$ is a filter of length N, and we should always have

$$\mathcal{F}\left(\mathbf{h}_{\mathrm{K},1}\right) \leq \mathcal{F}\left(\mathbf{h}_{\mathrm{K},2}\right) \leq \cdots \leq \mathcal{F}\left(\mathbf{h}_{\mathrm{K},N}\right). \tag{50}$$

The most interesting beamformer is derived from the maximization of the FBR. This leads to the the Krylov maximum FBR (KMFBR) beamformer:

$$\mathbf{h}_{\mathrm{KMFBR},N} = \frac{\mathbf{T}_N \mathbf{q}_{N,1}}{\mathbf{d}^H \mathbf{T}_N \mathbf{q}_{N,1}}, \tag{51}$$

where $\mathbf{q}_{N,1}$ is the eigenvector corresponding to the maximum eigenvalue of the matrix $\left(\mathbf{T}_N^H \mathbf{\Gamma}_{\pi/2,\pi} \mathbf{T}_N\right)^{-1} \left(\mathbf{T}_N^H \mathbf{\Gamma}_{0,\pi/2} \mathbf{T}_N\right)$.

The performance of the KMFBR beamformer also depends strongly on N.

1) For $N = 1$, we get $\mathbf{h}_{\mathrm{KMFBR},1} = \mathbf{i}_1$, where $\mathbf{i}_1$ is the first column of $\mathbf{I}_M$. This beamformer does not have any spatial gain. It simply selects the first sensor's signal as the beamformer's output.
2) For $N = M$, we get the supercardioid, i.e., $\mathbf{h}_{\mathrm{KMFBR},M} = \mathbf{h}_{\mathrm{SC}}$.
3) For $1 < N < M$, we obtain beamformers whose performances are in, general, between the performances of the all-pass filter (omnidirectional response) and the supercardioid.

As shown in simulations, the beamformer $\mathbf{h}_{\mathrm{KMFBR},N}$ can also find good compromises between large values of the FBR and reasonable values of the WNG.

VII. Parametric Superdirective Beamformer

As discussed in Section V, the columns of $\mathbf{K}_M$ are also good beamformers, where the first and last ones are the DS and superdirective beamformers, and the other columns are beamformers that can compromise between the WNG and the DF.

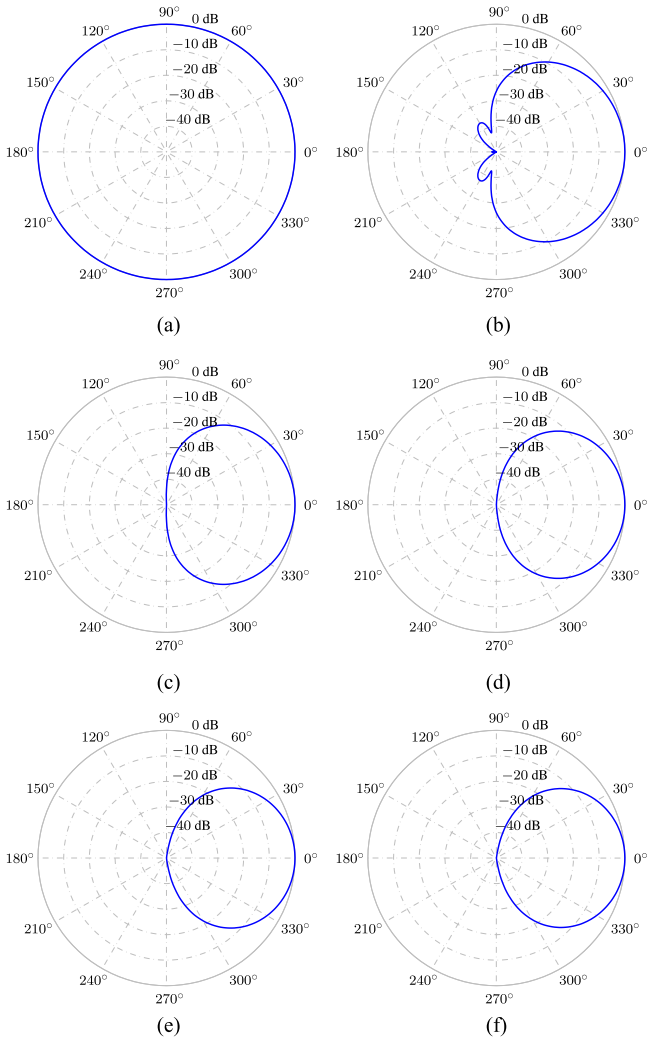

Fig. 3. Beampatterns of the KMFBR beamformer with a ULA, for six different values of N: (a) $N = 1$, (b) $N = 2$, (c) $N = 3$, (d) $N = 4$, (e) $N = 6$, and (f) $N = 8$. Conditions of simulation: $M = 8$, $\delta = 1.5$ cm, and $f = 2000$ Hz.

Consequently, any column of $\mathbf{K}_M$ can be rewritten as

$$\mathbf{h}_{\mathrm{P},p} = \frac{\boldsymbol{\Gamma}^{-\frac{1}{p}}\mathbf{d}}{\mathbf{d}^H\boldsymbol{\Gamma}^{-\frac{1}{p}}\mathbf{d}}, \tag{52}$$

where p is the parameter order, which takes values between between 1 and ∞, i.e., $p \in [1, \infty)$. We call $\mathbf{h}_{\mathrm{P},p}$ the parametric superdirective beamformer. As will become clearer soon, the value of p plays an important role in compromising between the DF and the WNG.

With the parametric superdirective beamformer, the WNG is

$$\mathcal{W}\left(\mathbf{h}_{\mathrm{P},p}\right) = \frac{\left|\mathbf{h}_{\mathrm{P},p}^H\mathbf{d}\right|^2}{\mathbf{h}_{\mathrm{P},p}^H\mathbf{h}_{\mathrm{P},p}} = \frac{\left(\mathbf{d}^H\boldsymbol{\Gamma}^{-\frac{1}{p}}\mathbf{d}\right)^2}{\mathbf{d}^H\boldsymbol{\Gamma}^{-\frac{2}{p}}\mathbf{d}}, \tag{53}$$

with

$$\mathcal{W}\left(\mathbf{h}_{\mathrm{P},1}\right) = \frac{\left(\mathbf{d}^H\boldsymbol{\Gamma}^{-1}\mathbf{d}\right)^2}{\mathbf{d}^H\boldsymbol{\Gamma}^{-2}\mathbf{d}} \leq M \tag{54}$$

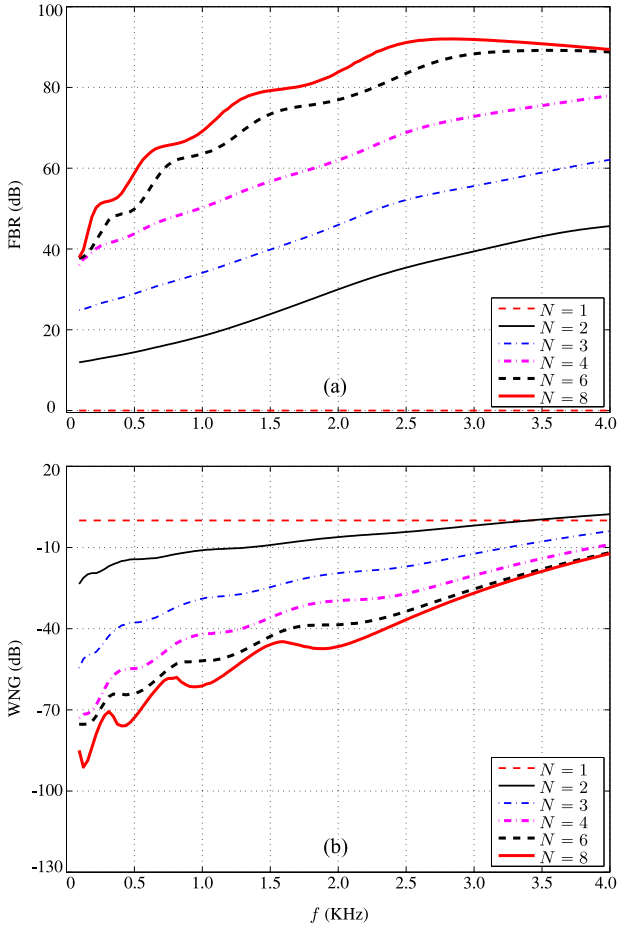

Fig. 4. FBR and WNG of the KMFBR beamformer with a ULA as a function of the frequency, f, for six different values of N: (a) FBR and (b) WNG. Conditions of simulation: $M = 8$ and $\delta = 1.5$ cm.

and

$$\mathcal{W}\left(\mathbf{h}_{\mathrm{P},\infty}\right) = M. \tag{55}$$

The DF with the proposed beamformer is

$$\mathcal{D}\left(\mathbf{h}_{\mathrm{P},p}\right) = \frac{\left|\mathbf{h}_{\mathrm{P},p}^H\mathbf{d}\right|^2}{\mathbf{h}_{\mathrm{P},p}^H\boldsymbol{\Gamma}\mathbf{h}_{\mathrm{P},p}} = \frac{\left(\mathbf{d}^H\boldsymbol{\Gamma}^{-\frac{1}{p}}\mathbf{d}\right)^2}{\mathbf{d}^H\boldsymbol{\Gamma}^{1-\frac{2}{p}}\mathbf{d}}, \tag{56}$$

with

$$\mathcal{D}\left(\mathbf{h}_{\mathrm{P},1}\right) = \mathbf{d}^H\boldsymbol{\Gamma}^{-1}\mathbf{d} \leq M^2 \tag{57}$$

and

$$\mathcal{D}\left(\mathbf{h}_{\mathrm{P},\infty}\right) = \frac{M^2}{\mathbf{d}^H\boldsymbol{\Gamma}\mathbf{d}} \geq 1. \tag{58}$$

For any given parameters $p_1 \geq p_2$, we should always have

$$\mathcal{W}\left(\mathbf{h}_{\mathrm{P},p_1}\right) \geq \mathcal{W}\left(\mathbf{h}_{\mathrm{P},p_2}\right) \tag{59}$$

and

$$\mathcal{D}\left(\mathbf{h}_{\mathrm{P},p_1}\right) \leq \mathcal{D}\left(\mathbf{h}_{\mathrm{P},p_2}\right). \tag{60}$$

Clearly, we obtain a beamformer whose DF decreases while WNG increases with p. So, by properly choosing the value of p, the parametric superdirective beamformer, $\mathbf{h}_{\mathrm{P},p}$, is able to

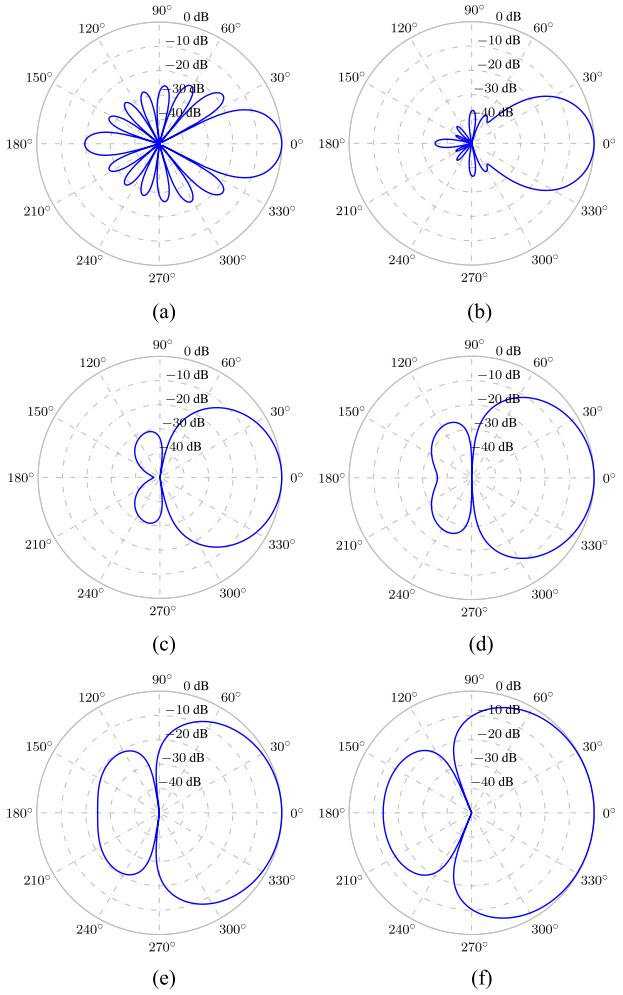

Fig. 5. Beampatterns of the parametric superdirective beamformer with a ULA, for six different values of the parameter order, p: (a) $p = 1$, (b) $p = 1.1$, (c) $p = 1.3$, (d) $p = 1.5$, (e) $p = 2$, and (f) $p = 10$. Conditions of simulation: $M = 8$, $\delta = 1.5$ cm, and $f = 2000$ Hz.

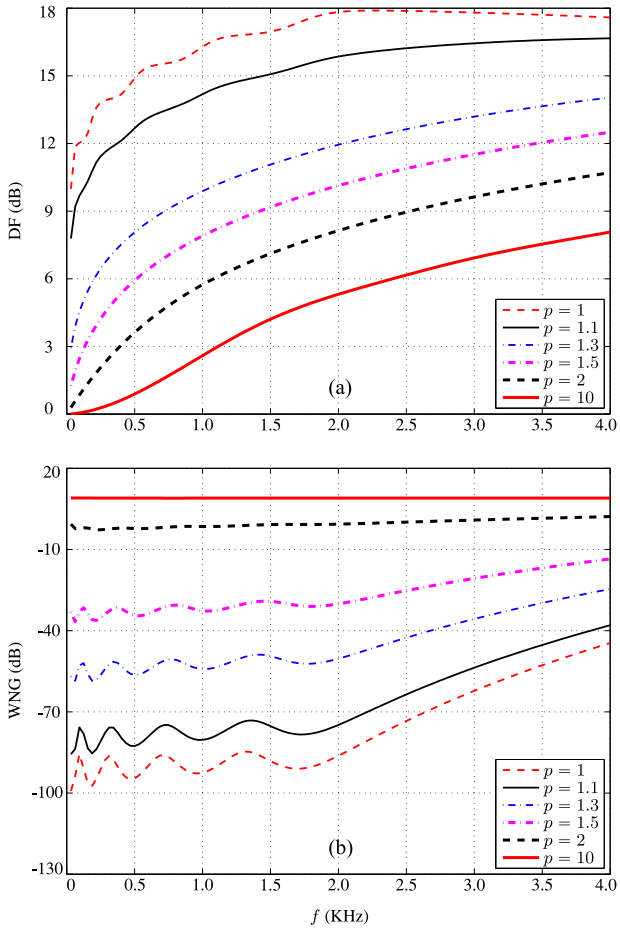

Fig. 6. DF and WNG of the parametric superdirective beamformer with a ULA as a function of the frequency, f, for six different values of the parameter order, p: (a) DF and (b) WNG. Conditions of simulation: $M = 8$ and $\delta = 1.5$ cm.

control white noise amplification while having a reasonably good value of the DF.

VIII. Parametric Supercardioid

From the decompositions in (44) and (45), it is easy to compute

$$\mathbf{\Gamma}_{0,\pi/2}^{\frac{1}{p}} = \mathbf{U}_1 \mathbf{\Lambda}_1^{\frac{1}{p}} \mathbf{U}_1^H, \tag{61}$$

$$\mathbf{\Gamma}_{\pi/2,\pi}^{\frac{1}{p}} = \mathbf{U}_2 \mathbf{\Lambda}_2^{\frac{1}{p}} \mathbf{U}_2^H, \tag{62}$$

where $p \in [1, \infty)$ is the parameter order. Denoting $\lambda_{p,1}$ the maximum eigenvalue of the matrix $\mathbf{\Gamma}_{\pi/2,\pi}^{-\frac{1}{p}} \mathbf{\Gamma}_{0,\pi/2}^{\frac{1}{p}}$ with $\mathbf{t}_{p,1}$ the corresponding eigenvector, and following the ideas of the previous section, we define the parametric supercardioid as

$$\mathbf{h}_{\mathrm{SC},p} = \frac{\mathbf{t}_{p,1}}{\mathbf{d}^H \mathbf{t}_{p,1}}. \tag{63}$$

The WNG with the parametric supercardioid is

$$\mathcal{W}\left(\mathbf{h}_{\mathrm{SC},p}\right) = \frac{\left|\mathbf{d}^H \mathbf{t}_{p,1}\right|^2}{\mathbf{t}_{p,1}^H \mathbf{t}_{p,1}}, \tag{64}$$

with

$$\mathcal{W}\left(\mathbf{h}_{\mathrm{SC},1}\right) = \frac{\left|\mathbf{d}^H \mathbf{t}_1\right|^2}{\mathbf{t}_1^H \mathbf{t}_1} \leq M \tag{65}$$

and

$$\mathcal{W}\left(\mathbf{h}_{\mathrm{SC},\infty}\right) = 1. \tag{66}$$

The FBR with the proposed beamformer is

$$\mathcal{F}\left(\mathbf{h}_{\mathrm{SC},p}\right) = \frac{\mathbf{t}_{p,1}^H \mathbf{\Gamma}_{0,\pi/2} \mathbf{t}_{p,1}}{\mathbf{t}_{p,1}^H \mathbf{\Gamma}_{\pi/2,\pi} \mathbf{t}_{p,1}}, \tag{67}$$

with

$$\mathcal{F}\left(\mathbf{h}_{\mathrm{SC},1}\right) = \lambda_1 \tag{68}$$

and

$$\mathcal{F}\left(\mathbf{h}_{\mathrm{SC},\infty}\right) = 1. \tag{69}$$

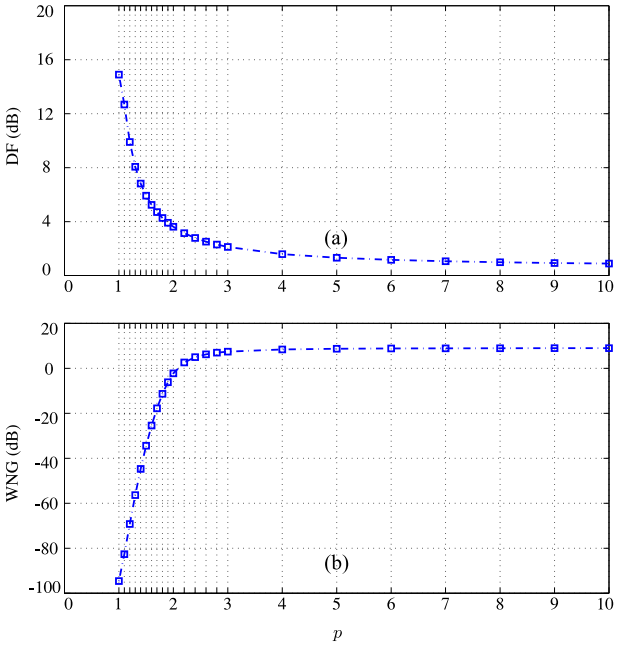

Fig. 7. DF and WNG of the parametric superdirective with a ULA as a function of the parameter order, p: (a) DF and (b) WNG. Conditions of simulation: $M = 8$, $\delta = 1.5$ cm, and $f = 1000$ Hz.

For any given parameters $p_1 \geq p_2$, we should always have

$$\mathcal{F}\left(\mathbf{h}_{\mathrm{SC},p_1}\right) \leq \mathcal{F}\left(\mathbf{h}_{\mathrm{SC},p_2}\right). \tag{70}$$

Clearly, the performance of the parametric supercardioid is also strongly influenced by the value of p.

IX. Simulations

In this section, we briefly study the performance of the proposed beamformers through simulations. We consider a ULA consisting of eight closely spaced microphones, with $\delta = 1.5$ cm. The desired signal impinges on the array from the endfire, i.e., $\theta = 0$, as discussed in Section II. The performance is evaluated with the beampattern, FBR, DF, and WNG. Both spherically isotropic noise and white noise are considered while all the superdirective beamformers are formed using the pseudo-coherence matrix given in (18).

A. Performance of the Krylov Superdirective Beamformer

We first study the performance of the Krylov superdirective beamformer. It is implemented according to (43).

Figure 1 plots the beampatterns of the KMDF beamformer (with $N = 1,\ 2,\ 3,\ 4,\ 6,\ 8$) for $f = 2000$ Hz. It is observed that the patterns vary greatly with N. For $N = 1$, we get the DS beampattern. For $N = 8$, we get the superdirective beampattern (or seventh-order hypercardioid). One can see that this beampattern has a one at the angle $\theta = 0^\circ$ and seven nulls in the range of 0° to 180°.

Figure 2 plots the DF and the WNG of the KMDF beamformer (with $N = 1,\ 2,\ 3,\ 4,\ 6,\ 8$) as a function of the frequency, f. It is seen that the superdirective beamformer ($N = 8$) achieves the maximum DF (approximately 18 dB). However, it suffers from significant white noise amplification, particularly at low frequencies, which limits its use in practice. For $N = 1$, we get the DS beamformer, which has the maximum WNG (approximately 9 dB) but its DF is low. In comparison, when N varies between 1 and 8, the KMDF beamformer achieves a good compromise between the performances of the DS and superdirective beamformers.

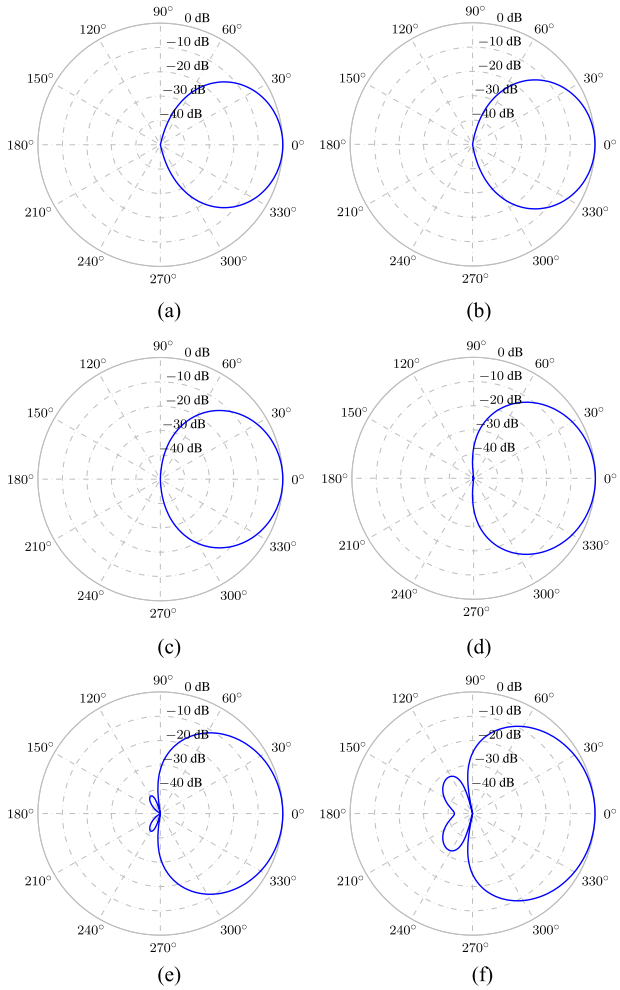

Fig. 8. Beampatterns of the parametric supercardioid with a ULA, for six different values of the parameter order, p: (a) $p = 1$, (b) $p = 1.5$, (c) $p = 2$, (d) $p = 3$, (e) $p = 4$, and (f) $p = 10$. Conditions of simulation: $M = 8$, $\delta = 1.5$ cm, and $f = 2000$ Hz.

B. Performance of the Krylov Supercardioid

In this simulation, we study the performance of the Krylov supercardioid. It is computed according to (51).

Figure 3 plots the beampatterns of the KMFBR beamformer (with $N = 1,\ 2,\ 3,\ 4,\ 6,\ 8$) for $f = 2000$ Hz. Again, the patterns vary greatly with N. For $N = 1$, it is the all-pass filter with an omnidirectional beampattern. For $N = 8$, it is the seventh-order supercardioid, whose beampattern has a large amplitude in the front-half plane (range from 0° to 90°) and a small amplitude in the rear-half plane (range from 90° to 270°).

The FBR and the WNG of the Krylov supercardioid (with $N = 1,\ 2,\ 3,\ 4,\ 6,\ 8$) as a function of frequency are plotted in Fig. 4. Clearly, the supercardioid beamformer ($N = 8$) has

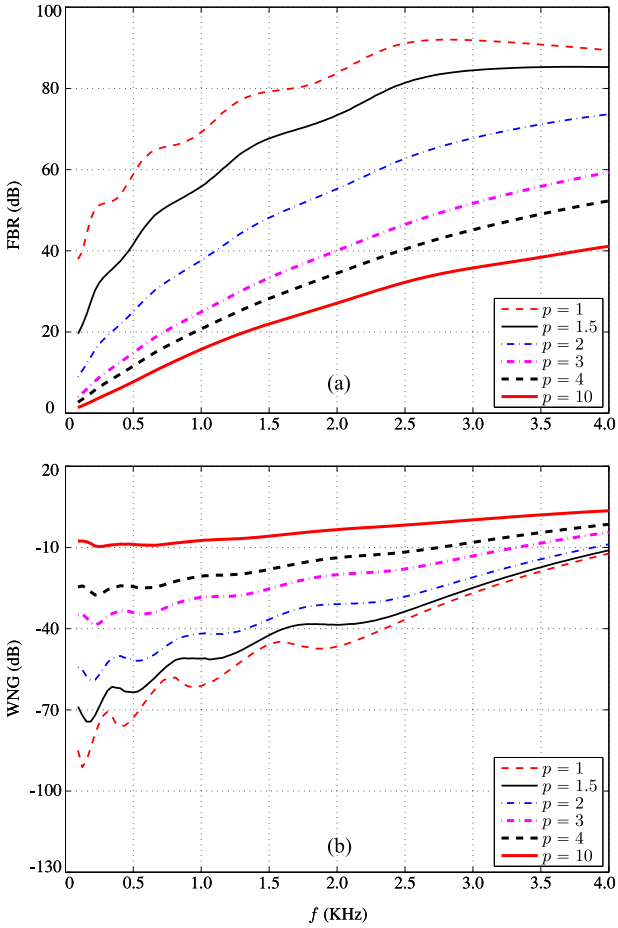

Fig. 9. FBR and WNG of the parametric supercardioid with a ULA as a function of the frequency, f, for six different values of the parameter order, p: (a) FBR and (b) WNG. Conditions of simulation: $M = 8$ and $\delta = 1.5$ cm.

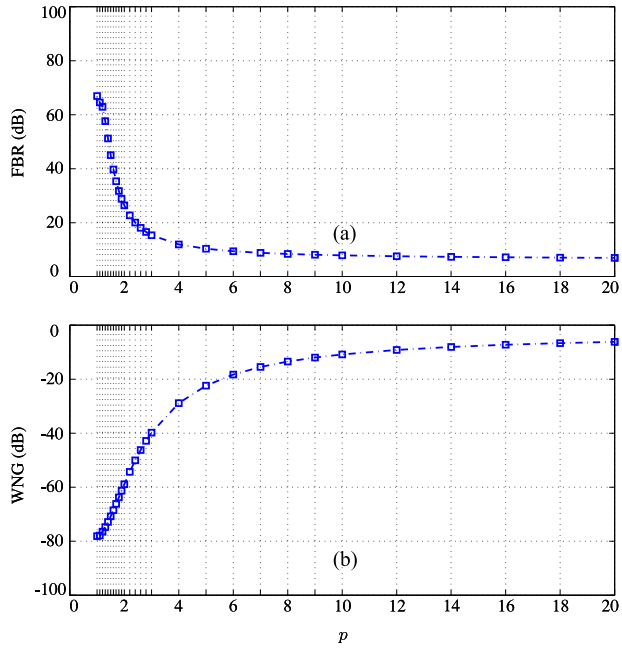

Fig. 10. FBR and WNG of the parametric supercardioid with a ULA as a function of the parameter order, p: (a) FBR and (b) WNG. Conditions of simulation: $M = 8$, $\delta = 1.5$ cm, and $f = 1000$ Hz.

tremendous white noise amplification at low frequencies even though the FBR is very high. These results are consistent with what was observed with the supercardioid. Not surprisingly, as the value of N increases, the value of the FBR becomes larger while the value of the WNG decreases. So, playing with the value of N, one can achieve a good compromise between large values of the FBR and white noise amplification with the KMFBR beamformer.

C. Performance of the Parametric Superdirective Beamformer

This subsection studies the performance of the parametric superdirective beamformer, which is computed according to (52).

Figure 5 plots the beampatterns of the parametric superdirective beamformer (with $p = 1,\ 1.1,\ 1.3,\ 1.5,\ 2,\ 10$) for $f = 2000$ Hz. As expected, the patterns vary greatly with p.

Figure 6 gives plots of the WNG and the DF of the parametric superdirective beamformer (with $p = 1,\ 1.1,\ 1,3,\ 1.5,\ 2,\ 10$) as a function of frequency. The case of $p = 1$ corresponds to the superdirective beamformer, which has a high value of the DF but suffers from significant white noise amplification. For $p = 10$, the beamformer resembles the DS beamformer, which has a large WNG but a low DF, especially at low frequencies. For $p = 1.1,\ 1.3,\ 1.5,\ 2$, the beamformer leads to lower values of the DF but higher values of the WNG.

It is noticed from Fig. 6 that the parameter order, p, plays a very important role on the beamforming performance. Figure 7 plots the DF and the WNG of the parametric superdirective beamformer as a function of p. It is seen that the DF decreases while the WNG increases significantly with p in the range between 1 to 3. When p is larger than 3, both the DF and the WNG do not vary much any more. Generally, we can choose a proper value of p within a small range to design a filter that can achieve a good compromise between the DF and the WNG.

D. Performance of the Parametric Supercardioid Beamformer

This last simulation studies the performance of the parametric supercardioid, which is implemented according to (63).

Figure 8 plots the beampatterns of the parametric supercardioid (with $p = 1,\ 1.5,\ 2,\ 3,\ 4,\ 10$) for $f = 2000$ Hz. Again, we see that the patterns vary greatly with p.

Finally, Figs. 9 and 10 plot the FBR and the WNG of the parametric supercardioid as a function of the frequency, f, and the parameter p, respectively. It is seen that the value of FBR decreases while the value of WNG increases significantly with p in the range from 1 to 6; but they both do not vary much if p is larger than 6. Consequently, by properly choosing p within a small range, this beamformer can also make a good compromise between FBR and WNG.

Note that both the Krylov and parametric beamformers can help control the compromise between the DF and the WNG. The major difference is that the former has only a small number (equal to the number of sensors) of choices in its parameter, and therefore it is easy to check what parameter is the best fit when given the array information. The latter, in contrast, is rather a

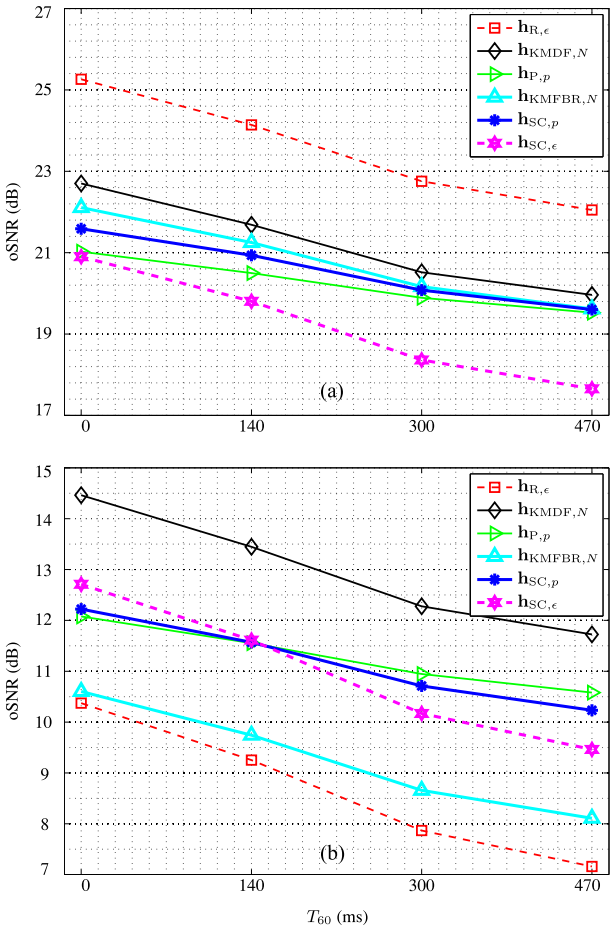

Fig. 11. Output SNR of the proposed beamformers with different reverberation conditions in (a) diffuse noise and (b) white Gaussian noise. Conditions of simulation: $M = 8$ and $\delta = 2.0$ cm.

general form with its parameter can change from 0 to infinity. Theoretically, this general form can provide more flexibility to deal with the white noise amplification problem; but tuning the optimal value may not be a trivial task and has to be performed separately at every frequency.

E. Performance in Reverberant Acoustic Environments

Now, we assess the performance of the developed beamformers in a more practical environment. We consider a room of size 4 m $\times$ 4 m $\times$ 3 m, where a linear array of 8 omnidirectional microphones are located, respectively, at $(x, 1.0, 2.5)$, where $x = 1.50 : 0.02 : 1.64$, and a loudspeaker is placed at $(2.5, 1.0, 1.5)$. The acoustic channel impulse responses from the source to the microphones are generated with the image model method [55]. Then, the microphone signals are generated by convolving the source signal (a speech signal prerecorded from a female speaker in a quiet office room) with the corresponding simulated impulse responses and some noise is then added to the result to control the SNR.

We consider two types of noise: white Gaussian noise and diffuse noise, both with an input SNR of 10 dB. We study four reverberation conditions where the room reflection coefficients are, respectively, 0, 0.6, 0.8, and 0.9 (the corresponding reverberation time T_{60} are approximately 0 ms, 140 ms, 300 ms, and 470 ms). All the signals are 30 seconds long and the sampling frequency is 16 kHz. We choose the first microphone as the reference. All the beamformers are implemented in the STFT domain with a frame size of 256 and a 256-point FFT (note that an overlapping factor of 75% is used and a Kaiser window is applied to each frame). To evaluate the overall performance, we use the fullband (0–4 kHz), time domain output SNR as the performance measure, which is computed using a long time average based on the 30-second long processed signals [56].

We present the regularized superdirective beamformer ($\mathbf{h}_{\mathrm{R},\epsilon}$, $\epsilon = 0.01$), the KMDF beamformer ($\mathbf{h}_{\mathrm{KMDF},N}$, $N = 2$), the parametric superdirective beamformer ($\mathbf{h}_{\mathrm{P},p}$, $p = 2$), the regularized supercardioid beamformer ($\mathbf{h}_{\mathrm{SC},\epsilon}$, $\epsilon = 0.01$), the KMFBR beamformer ($\mathbf{h}_{\mathrm{KMFBR},N}$, $N = 2$), and the parametric supercardioid beamformer ($\mathbf{h}_{\mathrm{SC},\epsilon}$, $p = 4$). The results are plotted in Fig. 11. It is seen that the superdirective beamformer with $\epsilon = 0.01$ yields the highest output SNR in diffuse noise, but lowest output SNR in white noise. The output SNR of the KMDF beamformer with $N = 2$ is approximately 2 dB lower than that of the regularized superdirective beamformer with $\epsilon = 0.01$ in diffuse noise; but it is about 5 dB higher than that of the regularized superdirective beamformer in white noise. Generally, all the studied beamformers behave differently in diffuse noise and white noise; but they all can achieve compromises by adjusting their parameters. In comparison, it is easy to find the best value of the parameter in the KMDF beamformer as there is only a small number of choices. Note that the optimal value of the parameters in every beamformer depends on practical situations and finding such value is beyond the scope of this paper.

X. Conclusion

The superdirective beamformer has been intensively studied for its ability to achieve maximum gains in diffuse noise. However, it is found to be very sensitive to sensor noise and mismatch among sensors, implying serious white noise amplification, especially at low frequency. Therefore, how to achieve a relatively high value of the DF with a reasonable value of the WNG has become an important issue regarding the design of beamformers with high gains. This paper developed an approach based on the Krylov matrix whose columns span a chosen dimension of the entire space. Linear combinations of any of the columns of this matrix also lead to different beamformers, the performances of which are in between the performances of the DS and superdirective beamformers. In particular, we developed the Krylov maximum white noise gain (KMWNG) and Krylov maximum DF (KMDF) beamformers, which are obtained by maximizing the WNG and the DF, respectively. By properly choosing the dimension of the Krylov subspace, which is easy in comparison with tuning the parameters in the so-called regularized superdirective beamformer, the KMDF beamformer can make a good compromise between a large value of the DF and a reasonable amount of white noise amplification. The basic idea was also extended to the design of supercardioid beamformers. Furthermore, we developed the parametric superdirective and supercardioid beamformers, which are special cases of the Krylov beamformers. Simulations demonstrated that the developed beamformers have interesting properties, which are useful for practical applications.

ACKNOWLEDGEMENTS

The authors would like to thank the associate editor and the three anonymous reviewers for their careful reading of the draft and providing many constructive comments and suggestions, which helped improve the clarity and quality of this paper.

REFERENCES

[1] H. Cox, R. M. Zeskind, and T. Kooij, "Practical supergain," *IEEE Trans. Acoust., Speech, Signal Process.*, vol. ASSP-34, no. 3, pp. 393–398, Jun. 1986.

[2] J. Capon, "High-resolution frequency-wavenumber spectrum analysis," *Proc. IEEE*, vol. 57, no. 8, pp. 1408–1418, Aug. 1969.

[3] G. W. Elko and J. Meyer, "Microphone arrays," in *Springer Handbook of Speech Processing*, J. Benesty, M. M. Sondhi, and Y. Huang, Eds.. Berlin, Germany: Springer-Verlag, 2008, ch. 48, pp. 1021–1041.

[4] I. Rakotoarisoa, J. Fischer, V. Valeau, D. Marx, C. Prax, and L.-E. Brizzi, "Time-domain delay-and-sum beamforming for time-reversal detection of intermittent acoustic sources in flows," *J. Acoust. Soc. Am.*, vol. 136, no. 5, pp. 2675–2686, 2014.

[5] H. Sun, W. Kellermann, E. Mabande, and K. Kowalczyk, "Localization of distinct reflections in rooms using spherical microphone array eigenbeam processing," *J. Acoust. Soc. Am.*, vol. 131, pp. 2828–2840, Apr. 2012.

[6] C. A. Anderson, P. D. Teal, and M. A. Poletti, "Spatially robust far-field beamforming using the von Mises (-Fisher) distribution," *IEEE/ACM Trans. Audio, Speech, Lang. Process.*, vol. 23, no. 12, pp. 2189–2197, Dec. 2015.

[7] S. Srinivasan, R. Aichner, B. Kleijn, and W. Kellermann, "Multichannel parametric speech enhancement," *IEEE Signal Process. Lett.*, vol. 13, no. 5, pp. 304–307, May 2006.

[8] Y. Huang, J. Chen, and J. Benesty, "Immersive audio schemes: The evolution of multiparty teleconferencing," *IEEE Signal Process. Mag.*, vol. 28, no. 1, pp. 20–32, Jan. 2011.

[9] J. Benesty, J. Chen, and Y. Huang, *Microphone Array Signal Processing*. Berlin, Germany: Springer-Verlag, 2008.

[10] S. Markovich, S. Gannot, and I. Cohen, "Multichannel eigenspace beamforming in a reverberant noisy environment with multiple interfering speech signals," *IEEE Trans. Audio, Speech, Lang. Process.*, vol. 17, no. 6, pp. 1071–1086, Aug. 2009.

[11] M. Brandstein and D. Ward, *Microphone Arrays Signal Processing–Techniques and Applications*. Berlin, Germany: Springer-Verlag, 2001.

[12] G. Huang, J. Benesty, T. Long, and J. Chen, "A family of maximum SNR filters for noise reduction," *IEEE/ACM Trans. Audio, Speech, Lang. Process.*, vol. 22, no. 12, pp. 2034–2047, Dec. 2014.

[13] B. Rafaely and D. Khaykin, "Optimal model-based beamforming and independent steering for spherical loudspeaker arrays," *IEEE Trans. Audio, Speech, Lang. Process.*, vol. 19, no. 7, pp. 2234–2238, Sep. 2011.

[14] A. Cigada, M. Lurati, F. Ripamonti, and M. Vanali, "Moving microphone arrays to reduce spatial aliasing in the beamforming technique: theoretical background and numerical investigation," *J. Acoust. Soc. Am.*, vol. 124, no. 6, pp. 3648–3658, 2008.

[15] F. Heese, M. Schafer, J. Wernerus, and P. Vary, "Numerical near field optimization of a non-uniform sub-band filter-and-sum beamformer," in *Proc. IEEE Int. Conf. Acoust., Speech Signal Process.*, 2013, pp. 96–100.

[16] H. W. Löllmann and P. Vary, "Post-filter design for superdirective beamformers with closely spaced microphones," in *Proc. IEEE Workshop Appl. Signal Process. Audio Acoust.*, 2007, pp. 291–294.

[17] H. Cox, R. Zeskind, and M. Owen, "Robust adaptive beamforming," *IEEE Trans. Acoust., Speech, Signal Process.*, vol. 35, no. 10, pp. 1365–1376, Oct. 1987.

[18] C. Bouchard, D. I. Havelock, and M. Bouchard, "Beamforming with microphone arrays for directional sources," *J. Acoust. Soc. Am.*, vol. 125, no. 4, pp. 2098–2104, 2009.

[19] S. Gannot, D. Burshtein, and E. Weinstein, "Beamforming methods for multi-channel speech enhancement," in *Proc. Int. Workshop Acoust. Signal Enhancement*, 1999, pp. 96–99.

[20] H. W. Löllmann and P. Vary, "Beamformer for driving binaural speech enhancement," in *Proc. Int. Workshop Acoust. Signal Enhancement*, 2012, pp. 1–4.

[21] B. Rafaely, "Phase-mode versus delay-and-sum spherical microphone array processing," *IEEE Signal Process. Lett.*, vol. 12, no. 10, pp. 713–716, Oct. 2005.

[22] Y. Zeng and R. C. Hendriks, "Distributed delay and sum beamformer for speech enhancement via randomized gossip," *IEEE/ACM Trans. Audio, Speech, Lang. Process.*, vol. 22, no. 1, pp. 260–273, Jan. 2014.

[23] O. L. Frost III, "An algorithm for linearly constrained adaptive array processing," *Proc. IEEE*, vol. 60, no. 8, pp. 926–935, Aug. 1972.

[24] M. Crocco and A. Trucco, "The synthesis of robust broadband beamformers for equally-spaced linear arrays," *J. Acoust. Soc. Am.*, vol. 128, no. 2, pp. 691–701, 2010.

[25] Y. Wang, Y. Yang, Y. Ma, and Z. He, "Robust high-order superdirectivity of circular sensor arrays," *J. Acoust. Soc. Am.*, vol. 136, no. 4, pp. 1712–1724, 2014.

[26] T. D. Abhayapala and A. Gupta, "Higher order differential-integral microphone arrays," *J. Acoust. Soc. Am.*, vol. 136, pp. 227–233, May 2010.

[27] J. Benesty and J. Chen, *Study and Design of Differential Microphone Arrays*. Berlin, Germany: Springer-Verlag, 2012.

[28] J. Chen, J. Benesty, and C. Pan, "On the design and implementation of linear differential microphone arrays," *J. Acoust. Soc. Am.*, vol. 136, no. 6, pp. 3097–3113, Dec. 2014.

[29] L. Zhao, J. Benesty, and J. Chen, "Design of robust differential microphone arrays," *IEEE/ACM Trans. Audio, Speech, Lang. Process.*, vol. 22, no. 10, pp. 1455–1466, Oct. 2014.

[30] M. Crocco and A. Trucco, "Design of robust superdirective arrays with a tunable tradeoff between directivity and frequency-invariance," *IEEE Trans. Signal Process.*, vol. 59, no. 5, pp. 2169–2181, May 2011.

[31] S. Yan, "Optimal design of modal beamformers for circular arrays," *J. Acoust. Soc. Am.*, vol. 138, no. 4, pp. 2140–2151, 2015.

[32] E. Tiana-Roig, F. Jacobsen, and E. Fernandez-Grande, "Beamforming with a circular array of microphones mounted on a rigid sphere (L)," *J. Acoust. Soc. Am.*, vol. 130, no. 3, pp. 1095–1098, 2011.

[33] S. Doclo and M. Moonen, "Superdirective beamforming robust against microphone mismatch," *IEEE Trans. Acoust., Speech, Signal Process.*, vol. 15, no. 2, pp. 617–631, Feb. 2007.

[34] T. Lotter and P. Vary, "Dual-channel speech enhancement by superdirective beamforming," *EURASIP J. Appl. Signal Process.*, vol. 2006, pp. 175–175, 2006.

[35] R. C. Hendriks and T. Gerkmann, "Noise correlation matrix estimation for multi-microphone speech enhancement," *IEEE/ACM Trans. Audio, Speech, Lang. Process.*, vol. 20, no. 1, pp. 223–233, Jan. 2012.

[36] E. Mabande, A. Schad, and W. Kellermann, "Design of robust superdirective beamformers as a convex optimization problem," in *Proc. IEEE Int. Conf. Acoust., Speech Signal Process.*, 2009, pp. 77–80.

[37] J. Bitzer and K. U. Simmer, "Superdirective microphone arrays," in *Microphone Arrays*. New York, NY, USA: Springer, 2001, pp. 19–38.

[38] G. W. Elko, "Superdirectional microphone arrays," in *Acoustic Signal Processing for Telecommunication*. New York, NY, USA: Springer, 2000, pp. 181–237.

[39] S. Shahbazpanahi, A. B. Gershman, Z.-Q. Luo, and K. M. Wong, "Robust adaptive beamforming for general-rank signal models," *IEEE Trans. Signal Process.*, vol. 51, no. 9, pp. 2257–2269, Sep. 2003.

[40] S. A. Vorobyov, A. B. Gershman, and Z.-Q. Luo, "Robust adaptive beamforming using worst-case performance optimization: A solution to the signal mismatch problem," *IEEE Trans. Signal Process.*, vol. 51, no. 2, pp. 313–324, Feb. 2003.

[41] J. Li, P. Stoica, and Z. Wang, "Doubly constrained robust Capon beamformer," *IEEE Trans. Signal Process.*, vol. 52, no. 9, pp. 2407–2423, Sep. 2004.

[42] J. Li, P. Stoica, and Z. Wang, "On robust Capon beamforming and diagonal loading," *IEEE Trans. Signal Process.*, vol. 51, no. 7, pp. 1702–1715, Jul. 2003.

[43] S. Gergen, N. Madhu, and R. Martin, "Performance characterization of linear arrays with respect to robust MVDR beamforming," in *Proc. Int. Workshop Acoust. Echo Noise Control*, 2010.

[44] R. Berkun, I. Cohen, and J. Benesty, "Combined beamformers for robust broadband regularized superdirective beamforming," *IEEE/ACM Trans. Audio, Speech, Lang. Process.*, vol. 23, no. 5, pp. 877–886, May 2015.

[45] C. Li, J. Benesty, G. Huang, and J. Chen, "Subspace superdirective beamformers based on joint diagonalization," in *Proc. IEEE Int. Conf. Acoust., Speech Signal Process.*, 2016, pp. 400–404.

[46] G. A. Seber, *A Matrix Handbook for Statisticians*. Hoboken, NJ, USA: Wiley, 2008.

[47] P. Kirsteins and H. Ge, "Performance analysis of Krylov space adaptive beamformers," in *Proc. IEEE Workshop Sensor Array Multichannel Process.*, 2006, pp. 16–20.

[48] H. Ruan and C. Rodrigo, "Robust adaptive beamforming based on low-rank and cross-correlation techniques," in *Proc. IEEE EUSIPCO*, 2015, pp. 854–858.

[49] D. Somasundaram and H. Parsons, "Robust Krylov-subspace methods for passive sonar adaptive beamforming," in *Proc. IMA Conf. Math. Defence*, 2013.
[50] D. Somasundaram, H. Parsons, P. Li, L. De, and C. Rodrigo, "Reduced-dimension robust Capon beamforming using Krylov-subspace techniques," *IEEE Trans. Aerosp., Elect., Syst.*, vol. 51, no. 1, pp. 270–289, Jan. 2015.
[51] C. Pan, J. Chen, and J. Benesty, "Performance study of the MVDR beamformer as a function of the source incident angle," *IEEE/ACM Trans. Audio, Speech, Lang. Process.*, vol. 22, no. 1, pp. 67–79, Jan. 2014.
[52] A. Uzkov, "An approach to the problem of optimum directive antenna design," *Comptes Rendus de l'Academie des Sci. de l'URSS*, vol. 53, pp. 35–38, 1946.
[53] G. H. Golub and C. F. V. Loan, *Matrix Computations*, 3rd ed. Baltimore, MD, USA: The Johns Hopkins Univ. Press, 1996.
[54] J. Benesty and T. Gänsler, "A multichannel acoustic echo canceler double-talk detector based on a normalized cross-correlation matrix," *Eur. Trans. Telecommun.*, vol. 13, no. 2, pp. 95–101, 2002.
[55] J. B. Allen and D. A. Berkley, "Image method for efficiently simulating smallroom acoustics," *J. Acoust. Soc. Am.*, vol. 65, pp. 943–950, Apr. 1979.
[56] J. Chen, J. Benesty, Y. Huang, and S. Doclo, "New insights into the noise reduction Wiener filter," *IEEE Trans. Audio, Speech, Lang. Process.*, vol. 14, no. 4, pp. 1218–1234, Jul. 2006.

Gongping Huang (S'13) received the Bachelor's degree in electronics and information engineering in 2012 from Northwestern Polytechnical University (NPU), Xi'an, China, where he is currently working toward the Ph.D. degree in information and communication engineering and also a visiting Ph.D. student at INRS-EMT, University of Quebec, Montreal, QC, Canada. His research interests include microphone array signal processing, noise reduction, speech enhancement, and audio and speech signal processing.

Jacob Benesty was born in 1963. He received the Master's degree in microwaves from Pierre & Marie Curie University, Paris, France, in 1987 and the Ph.D. degree in control and signal processing from Orsay University, Orsay, France, in April 1991.

During his Ph.D. (from November 1989 to April 1991), he worked on adaptive filters and fast algorithms at the Centre National d'Etudes des Telecomunications, Paris, France. From January 1994 to July 1995, he worked at Telecom Paris University on multichannel adaptive filters and acoustic echo cancelation. From October 1995 to May 2003, he was first a Consultant and then a Member of the Technical Staff at Bell Laboratories, Murray Hill, NJ, USA. In May 2003, he joined the University of Quebec, INRS-EMT, Montreal, QC, Canada, as a Professor. He is also a Visiting Professor at the Technion, Haifa, Israel, and an Adjunct Professor at Aalborg University, Denmark and at Northwestern Polytechnical University, Xi'an, China. His research interests include signal processing, acoustic signal processing, and multimedia communications. He is the Inventor of many important technologies. In particular, he was the Lead Researcher at Bell Labs who conceived and designed the world-first real-time hands-free full-duplex stereophonic teleconferencing system. Also, he conceived and designed the world-first PC-based multiparty hands-free full-duplex stereo conferencing system over IP networks.

Dr. Benesty was the Cochair of the 1999 International Workshop on Acoustic Echo and Noise Control and the General Cochair of the 2009 IEEE Workshop on Applications of Signal Processing to Audio and Acoustics. He received the IEEE Signal Processing Society 2001 Best Paper Award, with Morgan and Sondhi, and the IEEE Signal Processing Society 2008 Best Paper Award, with Chen, Huang, and Doclo. He is also the coauthor of a paper for which G. Huang received the IEEE Signal Processing Society 2002 Young Author Best Paper Award of a paper for which C. Pan received the IEEE R10 (Asia-Pacific Region) Distinguished Student Paper Award (First Prize) in 2016. In 2010, he received the Gheorghe Cartianu Award from the Romanian Academy. In 2011, he received the Best Paper Award from the IEEE WASPAA for a paper that he coauthored with J. Chen.

Jingdong Chen (M'99–SM'09) received the Ph.D. degree in pattern recognition and intelligence control from the Chinese Academy of Sciences, Beijing, China, in 1998.

From 1998 to 1999, he was with ATR Interpreting Telecommunications Research Laboratories, Kyoto, Japan, where he conducted research on speech synthesis, speech analysis, as well as objective measurements for evaluating speech synthesis. He then joined Griffith University, Brisbane, QLD, Australia, where he involved in research on robust speech recognition and signal processing. From 2000 to 2001, he worked at ATR Spoken Language Translation Research Laboratories on robust speech recognition and speech enhancement. From 2001 to 2009, he was a Member of Technical Staff at Bell Laboratories, Murray Hill, NJ, USA, working on acoustic signal processing for telecommunications. He subsequently joined WeVoice, Inc., in New Jersey, serving as the Chief Scientist. He is currently a Professor at Northwestern Polytechnical University, Xi'an, China. He coauthored the books *Fundamentals of Differential Beamforming* (Springer, 2016), *A Conceptual Framework for Noise Reduction* (Springer, 2015), *Design of Circular Differential Microphone Arrays* (Springer, 2015), *Study and Design of Differential Microphone Arrays* (Springer, 2013), *Speech Enhancement in the STFT Domain* (Springer, 2011), *Optimal Time-Domain Noise Reduction Filters: A Theoretical Study* (Springer, 2011), *Speech Enhancement in the Karhunen-Loève Expansion Domain* (Morgan Claypool, 2011), *Noise Reduction in Speech Processing* (Springer, 2009), *Microphone Array Signal Processing* (Springer, 2008), and *Acoustic MIMO Signal Processing* (Springer, 2006). He is also a coeditor/coauthor of the book *Speech Enhancement* (Berlin, Germany: Springer, 2005). His research interests include acoustic signal processing, adaptive signal processing, speech enhancement, adaptive noise/echo control, microphone array signal processing, signal separation, and speech communication.

Dr. Chen served as an Associate Editor of the IEEE TRANSACTIONS ON AUDIO, SPEECH, AND LANGUAGE PROCESSING from 2008 to 2014. He is currently a technical committee (TC) member of the IEEE Signal Processing Society (SPS) TC on Audio and Acoustic Signal Processing. He was the General Cochair of IWAENC 2016, the Technical Program Chair of IEEE TENCON 2013, a Technical Program Cochair of IEEE WASPAA 2009, IEEE ChinaSIP 2014, IEEE ICSPCC 2014, and IEEE ICSPCC 2015, and helped organize many other conferences.

He received the 2008 Best Paper Award from the IEEE Signal Processing Society (with Benesty, Huang, and Doclo), the Best Paper Award from the IEEE Workshop on Applications of Signal Processing to Audio and Acoustics (WASPAA) in 2011 (with Benesty), the Bell Labs Role Model Teamwork Award twice, respectively, in 2009 and 2007, the NASA Tech Brief Award twice, respectively, in 2010 and 2009, the Japan Trust International Research Grant from the Japan Key Technology Center in 1998, and the Young Author Best Paper Award from the 5th National Conference on Man–Machine Speech Communications in 1998. He is also the coauthor of a paper for which he received the IEEE R10 (Asia-Pacific Region) Distinguished Student Paper Award (First Prize) in 2016.